

# Self-assembling and Membrane Modifying Properties of a Lipopeptaibol Studied by CW-ESR and PELDOR Spectroscopies<sup>‡§</sup>

A. D. MILOV,<sup>α</sup> YU. D. TSVETKOV,<sup>α</sup> F. FORMAGGIO,<sup>β</sup> M. CRISMA,<sup>β</sup> C. TONIOLO<sup>β</sup> and J. RAAP<sup>γ</sup>

<sup>α</sup> Institute of Chemical Kinetics and Combustion, Novosibirsk, 630090 Russian Federation

<sup>β</sup> Institute of Biomolecular Chemistry, CNR, Department of Organic Chemistry, University of Padova, 35131 Padova, Italy

<sup>γ</sup> Leiden Institute of Chemistry, Gorlaeus Laboratories, Leiden University, 2300 RA Leiden, The Netherlands

Received 29 January 2003

Accepted 4 June 2003

**Abstract:** Trichogin GA IV is a short lipopeptaibol antibiotic that is capable of enhancing the transport of small cations through the phospholipid double layer of the membrane. The antibiotic activity of the undecapeptide is thought to be based on either its self-assembling or membrane-modifying property. The chemical equilibrium between self-aggregated and non-aggregated molecular states was studied by CW-ESR spectroscopy using solutions of TOAC nitroxide spin-labelled trichogin analogues in an apolar solvent to mimic the membrane bound state. At room temperature the two different sets of signals observed in the spectrum were attributed to the presence of both monomers and aggregates in the sample. The ESR spectra of the monomeric and aggregated forms were separated and the dependence of the fraction of monomeric peptide molecules on concentration was obtained over the range  $5 \times 10^{-6}$  to  $7 \times 10^{-4}$  M. A two-step aggregation mechanism is proposed: dimerization of peptide molecules followed by aggregation of dimers to assemblies of four peptide molecules per aggregate. The equilibrium constants were estimated for both steps. In addition, the lower lifetime limit was determined for dimers and tetramers. It is shown that when the peptide concentration exceeds  $10^{-5}$  M, the major part of the peptide molecules in solution has the form of tetrameric aggregates. Independently, the PELDOR technique was used to investigate the concentration dependence of the parameters of the dipole–dipole interaction between spin labels in frozen (77 K) glassy solutions of aggregates of mono-labelled TOAC analogues. The number of molecules in aggregates as well as the frequency and amplitude of PELDOR signal oscillations were found to be concentration independent in the range  $5 \times 10^{-4}$  to  $8 \times 10^{-3}$  M. In the frozen glassy solution state, the number of peptide molecules per aggregate was determined to be close to four, which is in agreement with the value obtained for spin-labelled trichogin at room temperature. The present data provide experimental evidence in favour of a self-assembling rather than a membrane-modifying ion conduction mechanism. Copyright © 2003 European Peptide Society and John Wiley & Sons, Ltd.

**Keywords:** aggregation; chemical equilibrium constants; membrane modifying peptaibol; spin-labelling

\*Correspondence to: Dr J. Raap, Leiden Institute of Chemistry, Leiden University, Einsteinweg 55, 2300RA Leiden, The Netherlands; e-mail: J.Raap@chem.LeidenUniv.nl

<sup>‡</sup> Presented at Peptaibols, October 2002, Jena, Germany.

<sup>§</sup> A part of this work was presented earlier in Milov AD, Tsvetkov YuD, Formaggio F, Crisma M, Toniolo C, Raap J. *A Workshop on Advanced EPR Applied to Biosciences, Satellite Symposium B in APES'01*. Kwansei: Japan, 2001; 99–108.

Contract/grant sponsor: Netherlands Organization of Scientific Research (NWO); Contract/grant number: 047-009-018.

Contract/grant sponsor: Russian Basic Science Research Foundation; Contract/grant numbers: 02-03-32022, 00-15-97321, 00-03-40124.

## INTRODUCTION

Trichogin GA IV is a member of the class of lipopeptaibol antibiotics and is characterized by the presence of an *n*-octanoyl (*n*Oct) group at the *N*-terminus and a leucinol (Lol) residue at the *C*-terminus of the linear undeca-peptide chain [1–3]. Recently, it has been shown that trichogin GA IV is capable of enhancing the conduction of monovalent cations through membranes of large unilamellar vesicles [4]. The number of lipopeptaibol molecules involved in the rate limiting step of ion diffusion is 3–4. However, the rate of ion conduction was found to be two orders of magnitude lower than those of typical ion channel forming peptaibols such as alamethicin and zervamicin. The length of the trichogin helical molecule is clearly too small to span the membrane bilayer so that the classical 'barrel-stave' mechanism of ion channel formation is unlikely. Concomitantly, CW (continuous wave)-ESR [5] and fluorescence quenching studies [6] indicated a parallel orientation of the trichogin helical axis with respect to the membrane surface. Its Gly-rich face is oriented toward the water layer and the hydrophobic face points toward the interior of the membrane, the octanoyl group probably anchoring the peptide molecule to the membrane surface ('carpet-like' mechanism [7,8]). In this model non-aggregated trichogin molecules are believed to diffuse at the membrane surface, thereby perturbing the local packing of the hydrophobic core of the membrane by insertion of the octanoyl chains. When molecules approach each other within a critical distance, the local distortions of the membrane structure will add up to transient opening of the bilayer creating hydrophilic paths for ion transport [9]. However, experimental evidence to support this model is still lacking and an ion carrier type of mechanism, e.g. that proposed for antimioebin [10], cannot be excluded.

More recently, the formation of aggregates of trichogin has been studied by Pulsed Electron Double Resonance (PELDOR) spectroscopy [11]. The self-assembling properties have been investigated in both polar and apolar solvents to mimic the two different local membrane environments, i.e. the polar head group–water interface and the apolar core of the phospholipid double layer. This is the technique of choice for determining intermolecular distances in the range 10–80 Å by accurate and quantitative analysis of the modulation phenomena of the PELDOR signal decays [12,13]. The application of PELDOR requires a frozen solution of spin-labelled

trichogin molecules in isotropic 'glassy' solvent systems. To this goal, three trichogin analogues, each with one of the three  $\alpha$ -aminoisobutyric acid (Aib) residues at positions 1, 4 and 8 of the amino acid sequence substituted by the conformationally rigid TOAC residue [14], a nitroxide spin- $C^{\alpha,\alpha}$ -dialkylated Gly, were synthesized. These replacements do not have any influence on the trichogin molecular 3D-structure, its ability to modify biological membranes and its antibiotic activity [15–17]. In solvents ranging from hydrophobic (decahydronaphthalene) to weakly polar (mixtures of chloroform–toluene), aggregates of peptide molecules are formed that dissociate upon addition of polar solvents such as alcohols [12,13]. The estimates based on experimental data testify that the observed aggregates contain about four peptide molecules and the *intermolecular* distances between TOAC1...TOAC1 and TOAC4...TOAC4 are 26.0 and 23.5 Å, respectively [12]. The results agree with a 'vesicular' model of the aggregate, wherein the four amphipathic  $3_{10}$ -type of peptide helices are oriented in an antiparallel fashion. The outside of the aggregate appears to be hydrophobic, whereas the inside of the cavity is polar. In a subsequent paper the secondary structure of the aggregated trichogin molecules was assessed by measuring the *intramolecular* distance between the two TOAC spin labels of the TOAC1,8 trichogin analogue [18].

Independently, the existence of aggregates was confirmed in both hydrophobic and weakly polar solvents at room temperature by CW-ESR spectroscopy [19]. From the corresponding hydrodynamic radii the calculated number of peptide molecules per aggregate agrees well with the previously observed value of 4 [12,17]. The CW-ESR spectral lines of the aggregates of the double-labelled peptide TOAC1,8 were found to be broader than those of non-aggregated peptide molecules and the correlation times of rotational mobility of aggregates and monomers were determined [19].

The possibility of separating the spectra of non-aggregated and aggregated forms of the double labelled TOAC1,8 trichogin analogue allowed a study of the chemical equilibrium of these forms in solution to be performed. The determination of the equilibrium constant made it possible to verify the possibility of aggregate formation in the membrane of vesicular systems. Also, the number of molecules per aggregate could be confirmed by considering the order of the aggregation reaction.

To ascertain the potential of this approach, CW-ESR spectra of TOAC1,8 trichogin in chloroform

solution at different concentrations were recorded at room temperature. The dependence of the fraction of non-aggregated molecules on peptide concentration was obtained for  $5 \times 10^{-6}$  M to  $7 \times 10^{-4}$  M concentrations. In this range the ESR spectrum varied from that of an almost non-aggregated peptide at low concentration to that of a fully aggregated peptide at high concentration. The basic structural parameters of the aggregates, i.e. the effective number of peptide molecules per aggregate and the distance between spin labels, were determined by analysing the amplitude and frequency of oscillations in the decay of the PELDOR signals in frozen glassy solutions [12,13]. However, there is no information available on the concentration dependence of these parameters.

This study focused attention on the concentration dependence of the parameters of the aggregates. Frozen glassy solutions of the TOAC1,8, TOAC1 and FTOAC4 trichogin analogues in a chloroform–toluene mixture were studied in detail using the PELDOR technique. The peptide concentration (from  $5 \times 10^{-4}$  to  $8 \times 10^{-3}$  M) widens the range used in previous studies of liquid solutions by CW-ESR.

The primary structures of trichogin GA IV and its spin-labelled analogues studied in this work are given below. In these peptides the C-terminal Lol was replaced by its synthetic precursor L-leucine methyl ester (Leu-OMe). In the FTOAC4 analogue the N-terminal *n*-octanoyl group was substituted by the Fmoc (9-fluorenylmethoxycarbonyl) moiety. None of these replacements alters the structural properties of trichogin [2,3]:

<i>n</i> Oct-Aib-Gly-Leu-Aib-Gly-Gly-Leu-Aib-Gly-Ile-Leu-Lol	(trichogin GA IV)
<i>n</i> Oct- <b>TOAC</b> -Gly-Leu-Aib-Gly-Gly-Leu- <b>TOAC</b> -Gly-Ile-Leu-Ome	(TOAC1,8)
<i>n</i> Oct- <b>TOAC</b> -Gly-Leu-Aib-Gly-Gly-Leu-Aib-Gly-Ile-Leu-Ome	(TOAC1)
Fmoc-Aib-Gly-Leu- <b>TOAC</b> -Gly-Gly-Leu-Aib-Gly-Ile-Leu-Ome	(FTOAC4)

## MATERIALS AND METHODS

The synthesis and characterization of the TOAC trichogin GA IV analogues have been previously described [15,16].

As in our previous studies [12,13], the magnetic dipole–dipole interaction in the aggregates of TOAC spin-labelled trichogin analogues in frozen solutions has been studied using the simplest variant of the PELDOR technique, based on the method of a two pulse electron spin echo at resonance frequency  $\nu_A$

with the addition of a pumping pulse at another frequency ( $\nu_B$ ) to turn over the portion of spins that takes no part in spin echo formation. The pumping pulse is applied between the two mw-pulses (forming the echo signal) at time  $T$  after the first pulse. The pumping pulse changes the sign of the dipole–dipole interaction between the spins forming the spin echo (spins A) and the spins excited by the pumping pulse (spins B). As a result, the spin echo amplitude starts to depend on both the position of pumping pulse  $T$  and the probability  $p_b$  of spins B flip induced by the pumping pulse. The study of the PELDOR signal dependence on  $T$  and  $p_b$  provides information on both the magnitude of dipole–dipole interaction between spin labels and the number of spin labels in aggregates. For further details the reader is referred to references [11] and [13].

The CW-ESR spectra of TOAC1,8 peptide solutions in chloroform were obtained at 20 °C using an ESP-380 Bruker spectrometer at a modulation frequency of 100 kHz and a modulation amplitude of 0.05 mT in the absence of spectral saturation. The samples for the ESR spectrometer (glass ampoules with a diameter of 0.3 cm) contained about 0.05 ml of a solution. As a solvent, spectrograde chloroform was used without additional purification. The TOAC1,8 peptide concentration varied from  $5 \times 10^{-6}$  M to  $7 \times 10^{-4}$  M.

The aggregates of peptides TOAC1 and FTOAC4 in frozen glassy solutions have been studied using a PELDOR spectrometer [13,20]. The durations of the first and second pulses forming the spin echo signal were 50 and 80 ns, respectively. The duration of

the pumping pulse was about 40 ns. The position of the pumping pulse corresponds to the maximum amplitude in the ESR spectrum. The difference in frequencies  $\nu_A - \nu_B$  was about 80 MHz. The  $p_b$  value, experimentally determined from the time dependence of PELDOR signal for the frozen glassy solutions of the double-labelled peptide TOAC1,8 in methanol [12], was found to be 0.2.

The samples for the PELDOR spectrometer were in the form of glass ampoules of 0.5 cm diameter containing about 0.08 ml of the solution studied.

As a solvent, chloroform–toluene mixture (7:3 by volume) was used giving transparent glassy specimens upon freezing in liquid nitrogen. The samples were placed in the finger of the Dewar flask cooled by liquid nitrogen located in the spectrometer resonator. The concentration of peptides varied from  $5 \times 10^{-4}$  M to  $8 \times 10^{-3}$  M. The lower concentration limit was controlled by the spectrometer sensitivity.

## RESULTS

### ESR Spectral Analysis

The ESR spectra of TOAC1,8 peptide solutions in chloroform at room temperature were similar to those obtained earlier [19]. The spectra were the sum of two nitroxyl triplets differing from one another for the widths of the individual components. According to reference [19], the broadened spectrum refers to the aggregates of TOAC1,8 molecules, whereas the triplet with relatively narrow components belongs to the TOAC1,8 non-aggregated molecules. The ratio between the two triplets in the spectrum depends on peptide concentration. In Figure 1, curves 1–3 illustrate the ESR spectra of TOAC1,8 peptide solutions depending on peptide concentration. Spectra 1–3 were normalized to the double integral value and for a convenient comparison, spectra 1 and 2 were multiplied by 4. As follows from Figure 1, the fraction of the narrow triplet in the spectrum increased with decreasing peptide concentration, thus indicating a shift in the chemical equilibrium towards the formation of non-aggregated TOAC1,8 molecules.

To determine the fraction of non-aggregated TOAC1,8 molecules in solution, the normalized experimental ESR spectrum  $I$  was represented as a sum of the spectra of aggregated and non-aggregated TOAC1,8 molecules

$$I = (1 - X_1)I_A + X_1I_N \quad (1)$$

where  $X_1$  is the fraction of non-aggregated TOAC1,8 molecules in solution (the ratio of the concentration of non-aggregated molecules to the total peptide concentration in solution), and  $I_A$  and  $I_N$  are the normalized spectra of aggregated and non-aggregated TOAC1,8 molecules, respectively.

The spectrum of non-aggregated molecules,  $I_N$ , was obtained by subtracting the spectra,  $I_1$  and

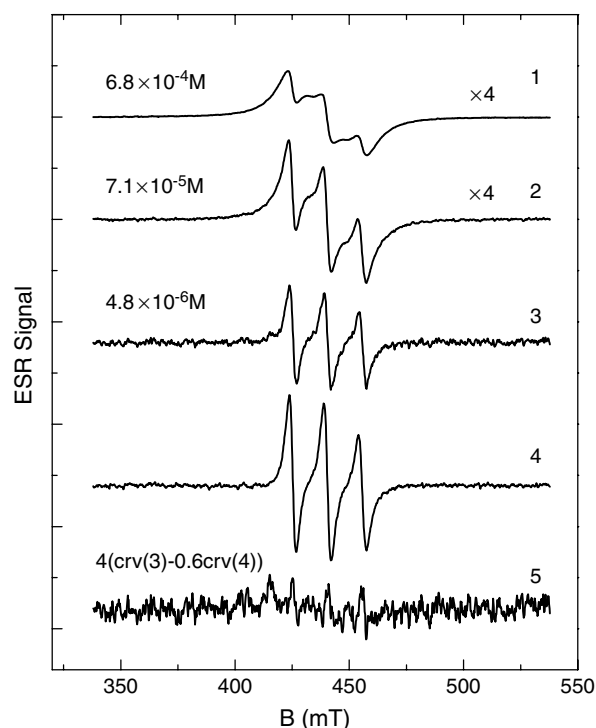


Figure 1 ESR spectra of peptide TOAC1,8 in chloroform at 20°C: curves 1–3 are the normalized spectra of peptide TOAC1,8 at the concentrations given in the Figure. Curve 4 is the normalized spectrum of non-aggregated TOAC1,8 molecules. Curve 5 is the difference spectrum of curves 3 and 4.

$I_2$ , for different total peptide concentrations from one another.

$$\Delta I = I_1 - \alpha I_2 = [(1 - X_{11}) - \alpha(1 - X_{12})]I_A + (X_{11} - \alpha X_{12})I_M \quad (2)$$

where  $\Delta I$  is the difference spectrum,  $X_{11}$  and  $X_{12}$  are the fractions of non-aggregated molecules corresponding to spectra  $I_1$  and  $I_2$ , respectively, and  $\alpha$  is the empirically chosen coefficient. Coefficient  $\alpha$  is taken so that the multiplier in front of  $I_A$  in Equation (2) is close to zero, i.e. the difference spectrum contains only the triplet with narrow components. In this case, according to Equation (2),  $I_N = \Delta I / (1 - \alpha)$  is obtained. The resulting spectrum  $I_N$ , averaged over several subtractions of different spectra and normalized, is shown in Figure 1 (curve 4).

Equation (1) and spectrum  $I_N$  were used to obtain the fraction of non-aggregated molecules  $X_1$ . The  $X_1I_N$  spectrum was subtracted from the experimental spectra by choosing the coefficient  $X_1$  so that the

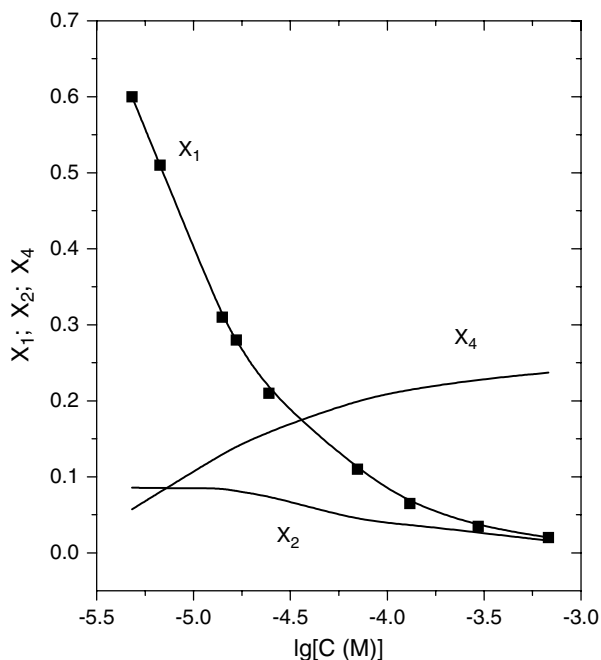


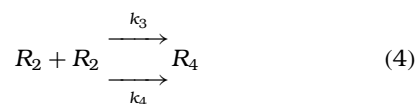
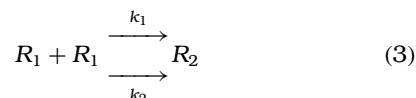
Figure 2 Dependence of fractions of non-aggregated peptide molecules  $X_1$ , dimers  $X_2$  and tetramers  $X_4$  upon TOAC1,8 peptide concentration ( $C$ ). For the experimental points for  $X_1$  and results of the calculations for  $X_2$  and  $X_4$  see text.

difference spectrum did not show any of the narrow components corresponding to spectrum  $I_N$ . For example, curve 5 in Figure 1 shows the difference between spectra 3 and 4 at  $X_1 = 0.6$ . The obtained dependence of fraction  $X_1$  of non-aggregated peptide molecules on the logarithm of the total peptide concentration  $C$  is given in Figure 2. The error in the determination of  $X_1$  is about 10%.

### Chemical Equilibrium of TOAC1,8 in Solution at Room Temperature

The aggregates of the trichogin GA IV analogues in weakly polar solvents contain about four peptide molecules [12,13,19]. To analyse the dependence of the fraction of non-aggregated TOAC1,8 molecules in chloroform solution on the peptide concentration (Figure 2), the simplest kinetic scheme was assumed in which dimers of peptide molecules might be formed in the first step of the aggregation process. In the second step, two dimers are assumed to aggregate to a cluster of four peptide molecules (tetramers). Denoting non-aggregated peptide molecules by  $R_1$ , and dimers and tetramers by  $R_2$  and  $R_4$ , respectively, the chemical equilibrium

schemes can be represented as



where  $k_i$  is the rate constant of the corresponding reaction. Denoting the concentration of component  $R_j$  in a solution by  $[R_j]$  and considering the concentrations to be time-independent, the solution to the kinetic schemes (3)–(4) at equilibrium conditions turns out to be

$$C - [R_1] = 2 \frac{k_1}{k_2} [R_1]^2 + 4 \left( \frac{k_1}{k_2} \right)^2 \frac{k_3}{k_4} [R_1]^4 \quad (5)$$

where  $C$  is the total concentration of spin-labelled peptide.

To analyse the experimental data, Equation (5) should be transformed by taking into account that  $[R_1] = X_1 C$

$$\frac{(1 - X_1)}{X_1^2 C} = 2 \frac{k_1}{k_2} + 4 \left( \frac{k_1}{k_2} \right)^2 \frac{k_3}{k_4} (X_1 C)^2. \quad (6)$$

If the above kinetic scheme is valid, then the experimental data, according to Equation (6), should give a straight line in the coordinates  $(1 - X_1)/(X_1^2 C)$  vs  $(CX_1)^2$ . In Figure 3 the experimental points are fit to a straight line within the limit of error. The line is drawn according to the least-square method. The slope of the line in Figure 3 is equal to  $4(k_1/k_2)^2(k_3/k_4) = (2 \pm 0.13) \times 10^{16} \text{ (LM}^{-1})^3$  and the intercept of the ordinate is  $2k_1/k_2 = (1.25 \pm 1.0) \times 10^5 \text{ (LM}^{-1})$ . These values make it possible to determine the equilibrium constants for both aggregation steps:  $k_1/k_2 = (0.62 \pm 0.5) \times 10^5 \text{ (LM}^{-1})$  and  $k_3/k_4 \approx 10^6 \text{ (LM}^{-1})$ . Because of the relatively big error in the determination of the  $k_1/k_2$  value, the  $k_3/k_4$  ratio can be estimated only as the order of the actual value. Thus, the obtained experimental data are in agreement with the proposed kinetic scheme of the formation of TOAC1,8 aggregates in chloroform.

In the framework of the above kinetic scheme, the ratio between the concentrations of tetramers  $[R_4]$  and dimers  $[R_2]$  depends on peptide concentration in  $C$  solution as follows

$$\frac{[R_4]}{[R_2]} = \frac{k_1 k_3}{k_2 k_4} (X_1 C)^2 \cong 8 \times 10^{10} (X_1 C)^2. \quad (7)$$

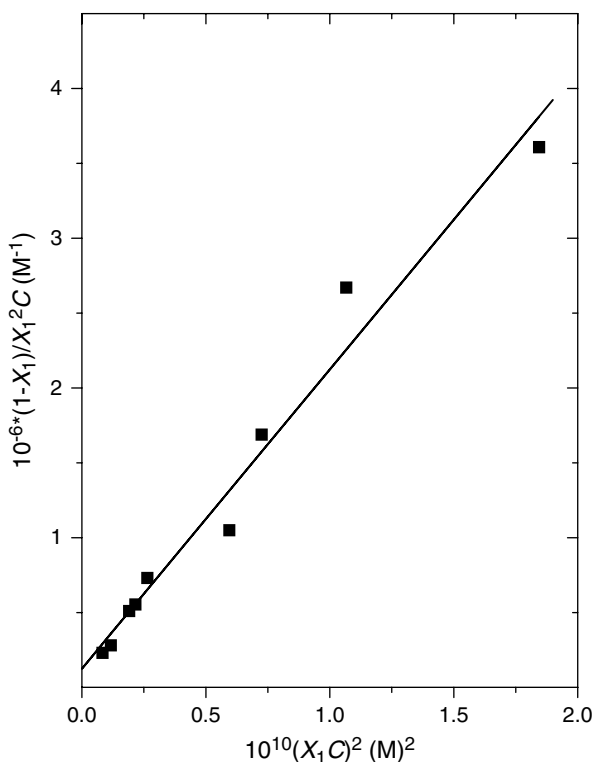


Figure 3 Linear representation of the experimental dependence of the fraction of non-aggregated TOAC1,8 molecules on concentration in chloroform according to Equation (6).

In the framework of the equilibrium schemes (3) and (4), taking into account the balance of the concentration condition  $4[R_4] + 2[R_2] + [R_1] = C$  and using Equation (7), it is possible to calculate the relative concentrations  $X_2 = [R_2]/C$  and  $X_4 = [R_4]/C$  as a function of the peptide concentration. The results of the  $X_2$  and  $X_4$  calculations, based on the ratios  $k_1/k_2$  and  $k_3/k_4$  obtained above, are shown in Figure 2 along with the experimental data for  $X_1$ . It follows from Figure 2 that at a peptide concentration of about  $6 \times 10^{-6}$  M the  $[R_4]/[R_2]$  ratio will be about unity. When the peptide concentration is increasing, the tetramer portion is also growing. Thus, when the peptide concentration in chloroform exceeds  $10^{-5}$  M, most of the peptide molecules are in the form of tetramers.

The values of ratios between the constants can be used to estimate the upper boundary of the lifetimes of dimers,  $\tau_2 = 1/k_2$  and tetramers,  $\tau_4 = 1/k_4$ . Taking into account that the constants  $k_1$  and  $k_3$  cannot exceed the values of the diffusion constant,  $k_D \approx 10^{10}$  ( $\text{LM}^{-1} \text{s}^{-1}$ ), from the above values for  $k_1/k_2$  and  $k_3/k_4$ ,  $\tau_2 =$

$0.62 \times 10^5/k_1 > 0.62 \times 10^5/k_D \approx 6 \times 10^{-6}$  s and  $\tau_4 \approx 10^6/k_3 > 10^6/k_D \approx 10^{-4}$  s is obtained.

Note that these values for the lower boundary of the lifetimes of aggregates are much higher than the time of rotational mobility of aggregates,  $10^{-9}$  s, obtained earlier [19]. Therefore, the processes of aggregate formation and decomposition have no considerable effect on the estimates of the correlation time of the rotational mobility, the distance between spin labels and their number in the aggregates [19].

### PELDOR Data at Different Concentrations of FTOAC4 and TOAC1 in Glassy Solutions at 77 K

The ESR spectra of the frozen glassy solution of peptides FTOAC4 and TOAC1 in the chloroform–toluene mixture are independent of the peptide concentration and coincide with those given previously [12,13]. Curves 1–3 in Figure 4, obtained at different concentrations of peptide FTOAC4, exemplify the experimental PELDOR signal decay  $V/V_0$  on the position of the pumping pulse  $T$ . In this case  $V_0$  is the value of signal  $V$  at  $T = 0$ . Figure 4 shows that at short times  $T$  (at  $T < 150$  ns), there is a fast decay in the PELDOR signal which is independent of the

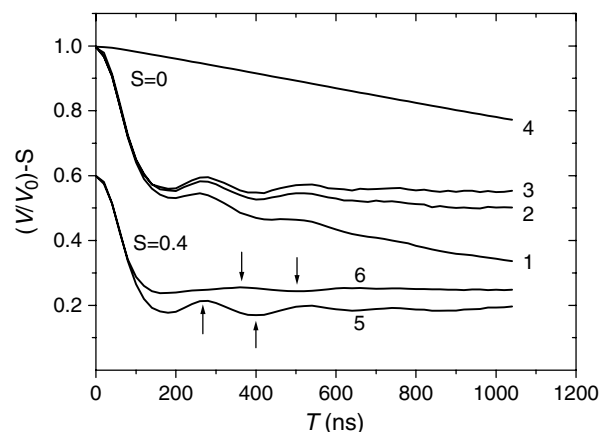


Figure 4 Experimental dependence of the PELDOR signal decay ( $V/V_0$ ) on time  $T$  for peptide FTOAC4 in chloroform–toluene mixture at 77 K at different concentrations. Curves 1–3 correspond to peptide FTOAC4 concentrations of  $8 \times 10^{-3}$  M,  $2 \times 10^{-3}$  M and  $0.5 \times 10^{-3}$  M, respectively. Curve 4 is the inter-aggregate contribution of spin labels for peptide FTOAC4. Curves 5 and 6 are the intra-aggregate contribution for peptides FTOAC4 and TOAC1, respectively. For convenience, the curves are shifted by the indicated value of  $S$ . The arrows on curves 5 and 6 show the minima and maxima of the modulation of the PELDOR decay.

peptide concentration. This fast decay is due to the relatively strong dipole–dipole interaction between the spin labels in the FTOAC4 peptide aggregates [14, 15]. A fast decay is followed by a slow one accompanied by oscillations and depends on the FTOAC4 peptide concentration. Under the same conditions, similar dependencies but with another frequency and oscillation amplitude are also observed for peptide TOAC4.

The dependence on peptide concentration of the PELDOR signal decay is due to the dipole–dipole interaction between spin labels belonging to different aggregates. Assuming, as in references [12] and [13], that the dipole–dipole interactions between spin labels in and between aggregates are independent of one another, the contributions of these interactions can be separated from the total dependence of  $V/V_0$  on  $T$ . In this case the dependence of  $V/V_0$  on  $T$  can be represented as the product of the PELDOR signal decay due to the intra-aggregate interaction between spin labels,  $V_{\text{INTRA}}$ , and the signal decay due to the inter-aggregate interaction between labels,  $V_{\text{INTER}}$ :  $V/V_0 = V_{\text{INTRA}} V_{\text{INTER}}$ .

According to reference [13], it is assumed that the dependence of the  $V_{\text{INTER}}$  value on the spin label concentration  $C$  is  $V_{\text{INTER}} = \exp(-p_b C f(T))$ , where  $p_b$  is the probability of spin flip induced by the pumping pulse and the function  $f(T)$  determines the dependence of  $V_{\text{INTER}}$  on time  $T$ . From the experimental dependencies of  $(V/V_0)_1$  and  $(V/V_0)_2$  on time  $T$  (obtained for the concentrations of the spin-labelled peptide,  $C_1$  and  $C_2$ , respectively) the dependencies of  $V_{\text{INTRA}}$  and  $V_{\text{INTER}}$  on  $T$  for a given concentration of  $C$  are

$$\ln(V_{\text{INTER}}) = C \ln((V/V_0)_2 / (V/V_0)_1) / (C_2 - C_1) \quad (8)$$

$$\ln(V_{\text{INTRA}}) = \ln((V/V_0)_1) - C_1 \ln((V/V_0)_2 / (V/V_0)_1) / (C_2 - C_1) \quad (9)$$

Equations (8) and (9) were used in reference [21] to separate the intra- and inter-aggregate interactions of spin labels when studying the spin-labelled analogues of trichogin. Figure 4 shows the dependencies of  $V_{\text{INTER}}$  (curve 4) and  $V_{\text{INTRA}}$  (curve 5) on time  $T$  obtained from Equations (8) and (9) for the FTOAC4 peptide aggregates. Curve 6 represents the dependence of  $V_{\text{INTRA}}$  on time  $T$  for TOAC1 obtained by the same method. For convenience, curves 5 and 6 are shifted downwards by the value  $S = 0.4$ . Curve 4 shows that the inter-aggregate interaction between spin labels leads to a smooth decay of the PELDOR signal. On the contrary, the interaction between spin

labels inside the aggregates (curves 5 and 6) leads to a fast decay of the signal  $V(T)$  at short times  $T$  followed by oscillations and the transition to a slow decay leading to the limiting value of  $V_p$  at longer times.

Figure 5 shows the dependencies of oscillation amplitudes  $\Delta V$  and  $V_p$  on the concentrations of peptides FTOAC4 and TOAC1. These parameters are independent of peptide concentration, at least in the range used in this study. The  $V_p$  values of FTOAC4 and TOAC1 are similar and coincide with those previously reported for a peptide concentration of about  $3 \times 10^{-3}$  M [13].

According to references [22] and [23], the  $V_p$  value is related to the distribution function over the number of spin labels per aggregate. The absence of the  $V_p$  dependence on peptide concentration indicates that in the concentration range studied the equilibrium is strongly shifted towards the formation of aggregates with a maximum number of peptide molecules and that the oscillations refer to dipole–dipole interactions between spin labels that are present inside the aggregates. The relatively small value of the oscillation amplitude  $\Delta V$  can be explained by a distribution over a range of distances between the labels in the aggregate, smoothing the dipole–dipole oscillations of the PELDOR signal [13].

When a sample contains aggregates with a different number of spin labels  $m$ , the  $V_p$  value is

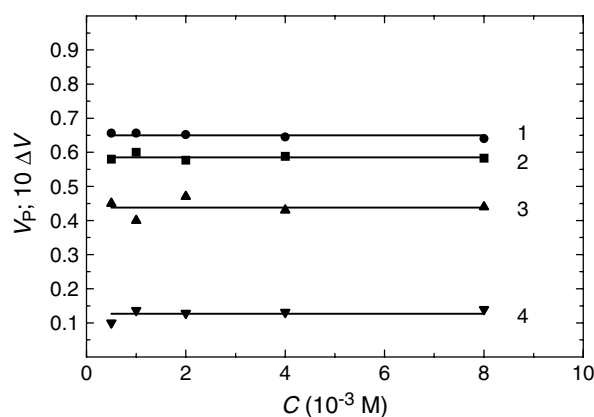


Figure 5 Dependence of the limiting decay value  $V_p$  and oscillation amplitude  $\Delta V$  on concentration for peptides FTOAC4 and TOAC1. Curves 1 and 2 refer to  $V_p$  for peptides TOAC1 and FTOAC4, respectively. Curves 3 and 4 refer to the oscillation amplitude  $\Delta V$  for peptides FTOAC4 and TOAC1, respectively. Oscillation amplitudes were measured as the difference in  $V/V_0$  values for curves 5 and 6 in Figure 4 at points denoted by arrows.

related to the  $m$ -distribution function via Equation (10) [20–22].

$$V_p = S_1/S_2 \quad (10)$$

with

$$S_1 = \sum_m G_m (1 - p_a)^{m-1} (1 - p_b)^{m-1} \quad (11)$$

$$S_2 = \sum_m G_m (1 - p_a)^{m-1} \quad (12)$$

where  $G_m$  is the fraction of spin labels belonging to aggregates containing  $m$  labels in their structures,  $p_a$  and  $p_b$  are the probabilities of spin flip induced by the second mw-pulse forming the echo and the pumping pulse, respectively. Summation in (11) and (12) is performed over  $m$  from 1 to the maximum number of spin labels per aggregate.

Equations (10)–(12) show that the shift in the chemical equilibrium with varying peptide concentration should lead to a change in the  $G_m$  value and thus to the dependence of  $V_p$  on the peptide concentration. The experimentally observed absence of dependence of  $V_p$  on concentration allows the assumption that in this case the equilibrium is fully shifted towards aggregated states and under these conditions aggregates of the same type are dominant in solution. For aggregates of the same type containing the same number  $N$  of spin labels it should be assumed that  $G_m = 0$  at  $m \neq N$  and  $G_N = 1$  (Equations (10) – (12)). In this case Equation (13) is operative:

$$V_p = (1 - p_b)^{N-1} \quad (13)$$

This equation makes it possible to estimate the number of spin labels per aggregate from known values of  $V_p$  and  $p_b$ . Substituting the  $V_p$  values obtained from Figure 5 and the experimental value of  $p_b$  into Equation (13), the  $N$  values for FTOAC4 and TOAC1, respectively, are obtained. Within the experimental error, the resulting values of  $N$  are close to 4, in agreement with the above kinetic scheme of aggregation in solutions, and  $N$  coincide with the previous estimates [11,12,21].

## DISCUSSION

It is essential to mention that the chosen kinetic scheme of aggregation is simplified and does not exclude the possibility of other pathways of aggregation, e.g. due to successive steps of aggregation, like

for instance: monomer→dimer→trimer→tetramer or the direct formation of tetramers from the fourth-order reaction of the monomer. However, the available experimental data are inadequate to distinguish among them with reasonable accuracy. In any case, when the peptide concentration in solution is above  $10^{-5}$  M, the major part of the peptide molecules is in the aggregated state. At higher concentrations the equilibrium shifts towards tetramer formation.

Comparing the data on the chemical equilibrium of aggregated and non-aggregated forms of the spin-labelled trichogin analogues in liquid solutions with the PELDOR data in frozen glassy solutions shows that with a further increase in peptide concentration to  $10^{-2}$  M the equilibrium fully shifts towards tetramer formation. The absence of concentration dependence of the  $V_p$  values supports the view that the process of aggregation is over at the stage of tetramer formation and that aggregates in which the number of molecules exceeds 4 are not formed.

The experimental values of  $N$  are slightly, but systematically, smaller than 4 [12]. Probably, such a decrease is caused by the method used to determine the  $p_b$  value. This parameter was calculated by assuming it is the convolution of the ESR absorption line with the pumping pulse parameters [13]. For systems with identical ESR spectra, the  $p_b$  values should also be equal. Taking into account that in frozen solutions the ESR spectra of aggregates and non-aggregated molecules (as it is in the double-labelled peptide TOAC1,8) are close to one another, the corresponding  $p_b$  values were assumed to be the same for these systems. The  $p_b$  value for peptide TOAC1,8 was determined from the experimental value of  $V_p$  from Equation (13) by taking into account that in this case  $N = 2$ . A minor systematic error (a decrease in  $N$ ) is possible due to the fact that the ESR spectra of TOAC1,8 aggregates can be characterized by an additional small broadening due to the dipole–dipole interaction between labels inside the aggregates.

## Biophysical Implications of the Equilibrium Data

Are the above equilibrium data relevant to understanding the mechanism of trichogin ion conduction that has been observed in membranes of liposomes and Gram-positive bacterial cells? [4,24]. Figure 2 shows that in hydrophobic solvents tetramers are present in the concentration range between  $10 \mu\text{M}$  and  $1 \text{mM}$ . However, the minimal concentration of trichogin able to promote ion conductance through vesicular membranes is slightly lower, i.e. in the



order of  $\mu\text{M}$  [4]. To understand this difference, one has to take into account that in a typical ion conduction experiment a few  $\mu\text{l}$  of dimethylsulphoxide solution of trichogin is added to a 2 ml volume of an aqueous vesicle suspension with a lipid concentration of 200  $\mu\text{M}$ . Under these conditions the lipophilic peptide is almost quantitatively bound to the membrane [25]. This means that the local concentration of trichogin in the partial volume of the aqueous suspension occupied by vesicles is about three orders of magnitude higher than the total concentration.

In another experiment, that has been described elsewhere [26], a spin-labelled trichogin analogue was added to a suspension of bacterial cells. After centrifugation the CW-ESR spectrum of the supernatant did not show any residual CW-ESR signal. From a comparison of the PELDOR decay curves of the spin-labelled trichogin in the monomeric state and in the membrane-bound state it was concluded that the local concentration of the trichogin bound molecules is at least a factor of 10 higher than the average concentration [24]. However, in spite of the fact that addition of trichogin to the bacterial suspension leads to the efflux of  $\text{K}^+$  ions, indicating that this peptaibol acts in bacterial membranes similar to vesicular phospholipid double layers, no aggregation of molecules was found. Instead, unaggregated molecules are distributed at the cytoplasmic membrane [24].

Clearly, the trichogin membrane-bound state, wherein monomeric molecules lay parallel to the surface as in liposomes [16], seems to be the thermodynamically most stable state. Thus, aggregates of surface bound molecules, as in the carpet-like model, are not thermodynamically stable. Moreover, atomic force microscopy experiments did not show any peptide induced detergent-like disintegration or phase transition of the planar phospholipid double layer even at a lipid to peptide ratio of 9 (unpublished data).

The in-plane bound state has been proposed for many other peptaibols that are too short to span the phospholipid membrane. For instance, solid-state NMR studies of the 16-peptide zervamicin bound to 1,2-dioleoyl-*sn*-glycero-3-phosphocholine (DOPC, a di-C18:1-PC) double layer shows an in-plane orientation, while under the same condition the 20-mer alamethicin displays a transmembrane orientation [26]. However, zervamicin forms a transmembrane orientation when it is bound to the thinner di-C10:0-PC. This phenomenon has been explained in terms of a topological equilibrium between the two different bound states. In DOPC the 16-mer peptide is slightly

too short to match the thickness of the hydrophobic core of the membrane. However, the existence of such an equilibrium is not plausible for the case of the trichogin bound state since this lipopeptaibol can only span half of the double layer at maximum.

From the kinetics of the ion conduction experiments it is known that four molecules of trichogin are involved in the rate limiting step [4]. Thus, most likely, trichogin molecules form metastable tetramers after penetration of the amphipathic molecules into the hydrophobic core of the double layer, thereby entrapping ions into the polar cavity of the tetramer (Figure 6). After diffusion from the

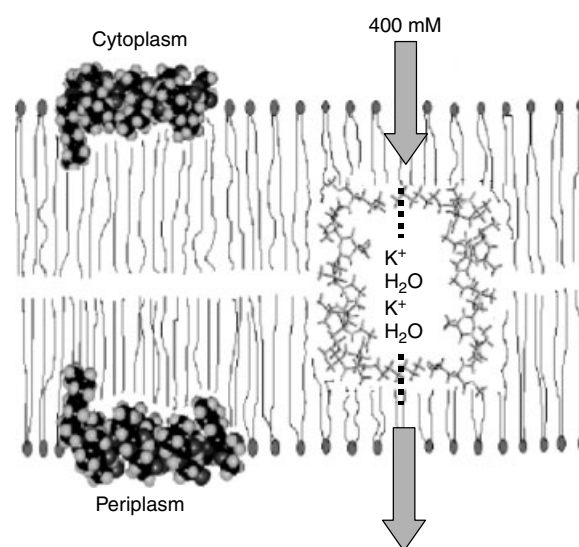


Figure 6 Schematic model of the trichogin-induced ion conduction through phospholipid double layers. The thermodynamically most stable binding state is the monomeric molecule bound at the surface of the membrane. Formation of tetramers might be driven by the presence of the electrochemical gradient that exists over the membrane. For clarity, only the cross-section of the tetramer is shown, i.e. the initially formed dimer, with antiparallel oriented peptide chains and with the polar sides of the amphipathic molecules facing towards each other. The tetramer is formed by aggregation of two dimers. The structure of the second dimer of the tetramer (not shown) is created from the first one by rotation of  $90^\circ$  around the axis intersecting the *n*Oct/*L*ol side chains (dashed line). The two ends of the tetrameric aggregate are closed by the presence of the bulky terminal *n*Oct/*L*ol side chains. In this way a polar cavity is formed inside the aggregate, whereas the outside appears to be hydrophobic. During aggregation, the solvated ions can be entrapped into the polar pocket of the aggregate which will be released after diffusion of the vesicle to the other side of the membrane with concomitant dissociation of the tetramer at the polar head group region.

periplasmic to the cytoplasmic bound states and *vice versa* the ions will be released by dissociation of the tetramers upon approaching the interface between the hydrophobic core and the polar head group region of the membrane.

Previous liposome studies suggested that the trichogin induced ion transport has a slightly favoured selectivity for  $K^+$  ions compared with  $Na^+$  ions [4]. The preferential permeation of  $K^+$  ions over  $Na^+$  ions matches the difference between ion radii of the hydrated ions ( $rK^+_{aq} < rNa^+_{aq}$ ) and parallels the tendency found by passive ion diffusion through statistically distributed and water filled pores in pure lipid bilayers [27]. However, fluorescence experiments with vesicles loaded with a highly concentrated KCl solution, did not exhibit any cation selectivity like that shown by the  $K^+$ -specific ion-carrier valinomycin. Thus, trichogin does not act as a cation specific ion carrier and for this reason the 'vesicular' ion conduction model was proposed [12].

## CONCLUSIONS

The CW-ESR method was used to study the equilibrium between monomers and the aggregates of the spin-labelled peptide TOAC1,8 in chloroform at room temperature. The dependence of the fraction of monomeric molecules on peptide concentration in solution was obtained by separating the ESR spectra of aggregated and monomeric forms. It is shown that this dependence is described by a two-step kinetic scheme, i.e. dimerization of monomeric peptide molecules with subsequent combination of dimers into tetramers. The values of the equilibrium constants of dimerization were estimated to be  $0.6 \times 10^5$  ( $LM^{-1}$ ) and those of tetramer formation from dimers were estimated to be about  $10^6$  ( $LM^{-1}$ ). The lower boundaries of the lifetimes of dimers and tetramers were determined to be  $6 \times 10^{-6}$  s and  $10^{-4}$  s, respectively. When the peptide concentration is above  $10^{-5}$  M, the concentration of tetramers in solution exceeds that of dimers. The PELDOR technique was used to study the dependence of oscillation amplitude and PELDOR signal decay on peptide concentration in frozen glassy solution (77 K). The contributions of *intra*-aggregate and *inter*-aggregate interactions between spin labels to the time dependence of the PELDOR signal were separated. In the peptide concentration range  $5 \times 10^{-4}$  M to  $8 \times 10^{-3}$  M the oscillation amplitude and PELDOR signal decay are independent of the peptide concentration due to the dipole-dipole

interaction between spin labels in the aggregate that corresponds to the almost complete shift of the equilibrium toward the formation of aggregates containing four peptide molecules per aggregate. The results are discussed in terms of a proposed vesicular model.

## Acknowledgements

The research described in this publication was made possible in part by the Netherlands Organization of Scientific Research (NWO), project 047-009-018 and the Russian Basic Science Research Foundation, grants 02-03-32022, 00-15-97321 and 00-03-40124.

## REFERENCES

1. Rebuffat S, Goulard Ch, Bodo B, Roquebert MF. The peptaibol antibiotics from *Trichoderma* fungi. Structural diversity and membrane properties. *Rec. Res. Dev. Org. Bioorg. Chem.* 1999; **3**: 65–91.
2. Toniolo C, Crisma M, Formaggio F, Peggion C, Epand RF, Epand RM. Lipopeptaibols, a novel family of membrane active, antimicrobial peptides. *Cell. Mol. Life Sci.* 2001; **58**: 1179–1188.
3. Peggion C, Formaggio F, Crisma M, Epand RF, Epand RM, Toniolo C. Trichogin: a paradigm for lipopeptaibols. *J. Pept. Sci.* 2003; **9**: 679–689.
4. Kropacheva TN, Raap J. Ion transport across a phospholipid membrane mediated by the peptide trichogin GA IV. *Biochim. Biophys. Acta* 2002; **1567**: 193–203.
5. Monaco V, Formaggio F, Crisma M, Toniolo C, Hanson P, Millhauser GL. Orientation and immersion depth of a helical lipopeptaibol in membranes using TOAC as an ESR probe. *Biopolymers* 1999; **50**: 239–253.
6. Epand RF, Epand RM, Monaco V, Stoia S, Formaggio F, Crisma M, Wu H, Lehrer RI, Toniolo C. Analogs of the antimicrobial peptide trichogin having opposite membrane properties. *Eur. J. Biochem.* 1999; **266**: 1021–1028.
7. Pouny Y, Rapaport A, Nicolas P, Shai Y. Interaction of antimicrobial dermaseptin and its fluorescently labeled analogs with phospholipid membranes. *Biochemistry* 1992; **31**: 12 416–12 423.
8. Epand RM, Shai Y, Segrest JP, Anantharamaiah GM. Mechanisms for the modulation of membrane bilayer properties by amphipathic helical peptides. *Biopolymers* 1999; **37**: 319–338.
9. Bechinger B. The structure, dynamics and orientation of antimicrobial peptides in membranes by

- multidimensional solid-state NMR spectroscopy. *J. Membrane Biol.* 1997; **156**: 197–211.
10. Snook CF, Woolley GA, Oliva G, Pattabhi V, Wood SP, Blundell TL, Wallace BA. The structure and function of antiameobin I, a proline-rich membrane-active polypeptide. *Structure* 1998; **6**: 783–792.
  11. Milov AD, Maryasov AG, Tsvetkov YuD. Pulsed electron double resonance (PELDOR) and its application in free-radicals research. *Appl. Magn. Reson.* 1998; **15**: 107–143.
  12. Milov AD, Tsvetkov YuD, Formaggio F, Crisma M, Toniolo C, Raap J. Self-assembling properties of membrane-modifying peptides studied by PELDOR and CW-ESR spectroscopies. *J. Am. Chem. Soc.* 2000; **122**: 3843–3848.
  13. Milov AD, Tsvetkov YuD, Raap J. Aggregation of trichogin analogs in weakly polar solvents: PELDOR and ESR studies. *Appl. Magn. Reson.* 2000; **19**: 215–227.
  14. Toniolo C, Crisma M, Formaggio F. TOAC: a nitroxide spin-labeled, achiral, C<sup>α</sup>-tetrasubstituted  $\alpha$ -amino acid, is an excellent tool in materials science and biochemistry. *Biopolymers (Pept. Sci.)* 1998; **47**: 153–158.
  15. Monaco V, Formaggio F, Crisma M, Toniolo C, Hanson P, Millhauser G, George C, Deschamps JR, Flippen-Anderson JL. Determining the occurrence of a  $3_{10}$ -helix and an  $\alpha$ -helix in two different segments of a lipopeptaibol antibiotic using TOAC, a nitroxide spin-labeled C<sup>α</sup>-tetrasubstituted  $\alpha$ -amino acid. *Bioorg. Med. Chem.* 1999; **7**: 119–131.
  16. Monaco V, Formaggio F, Crisma M, Toniolo C, Hanson P, Millhauser G. Orientation and immersion depth of a helical lipopeptaibol in membranes using TOAC as an ESR probe. *Biopolymers* 1999; **50**: 239–253.
  17. Toniolo C, Crisma M, Formaggio F, Peggion C, Monaco V, Goulard C, Rebuffat S, Bodo B. Effect of N<sup>α</sup>-acyl chain length on the membrane-modifying properties of synthetic analogs of the lipopeptaibol trichogin GA IV. *J. Am. Chem. Soc.* 1996; **118**: 4952–4958.
  18. Milov AD, Tsvetkov YuD, Formaggio F, Crisma M, Toniolo C, Raap J. The secondary structure of a membrane-modifying peptide in a supramolecular assembly studied by PELDOR and CW-ESR spectroscopies. *J. Am. Chem. Soc.* 2001; **123**: 3784–3789.
  19. Milov AD, Tsvetkov YuD, Formaggio F, Crisma M, Toniolo C, Millhauser GL, Raap J. Self-assembling properties of a membrane modifying lipopeptaibol in weakly polar solvents studied by CW-ESR. *J. Phys. Chem.* 2001; **105**: 11 206–11 213.
  20. Milov AD, Salikhov KM, Schirov MD. *Fiz. Tverd. Tela. (Russ.)* 1981; **23**: 975–982.
  21. Milov AD, Maryasov AG, Tsvetkov YuD, Raap J. Pulsed ELDOR in spin-labelled polypeptides. *Chem. Phys. Lett.* 1999; **303**: 135–143.
  22. Milov AD, Ponomarev AB, Tsvetkov YuD. Electron-electron double resonance in electron spin-echo: model biradical systems and the sensitized photolysis of decalin. *Chem. Phys. Lett.* 1984; **110**: 67–72.
  23. Ponomarev AB, Milov AD, Tsvetkov YuD. *Khim. Fiz. (Russ.)* 1988; **7**: 1673–1680.
  24. Milov AD, Samoilova RI, Tsvetkov YuD, Gusev VA, Formaggio F, Crisma M, Toniolo C, Raap J. Spatial distribution of spin-labelled trichogin GA IV in the Gram-positive bacterial cell membrane determined from PELDOR data. *Appl. Magn. Reson.* 2002; **23**: 81–95.
  25. Stella L, Mazzuca C, Palleschi A, Venanzi M, Formaggio F, Toniolo C, Moroder L, Pispisa B. Mechanism of membrane permeabilization by the lipopeptaibol trichogin GA IV and its fluorescent analogues. In *Peptides 2002, Proceedings of the 27th Europeptide Symposium, Italy*, Benedetti E (ed.). 894–895.
  26. Bechinger B, Skladnev AA, Ogrel A, Li X, Rogozhkina EV, Ovchinnikova TV, O'Neil JDJ, Raap J. <sup>15</sup>N and <sup>31</sup>P solid-state NMR investigations on the orientation of zervamicin II and alamethicin in phosphatidylcholine membranes. *Biochemistry* 2001; **40**: 9428–9437.
  27. Deamer DW, Bramhall J. Permeability of lipid bilayers to water and ionic solutes. *Chem. Phys. Lipids* 1986; **40**: 167–188.